We are IntechOpen, the world's leading publisher of Open Access books Built by scientists, for scientists

6,900
Open access books available

185,000
International authors and editors

200M
Downloads

Our authors are among the

154
Countries delivered to

TOP 1%
most cited scientists

12.2%
Contributors from top 500 universities



WEB OF SCIENCE™

Selection of our books indexed in the Book Citation Index in Web of Science™ Core Collection (BKCI)

Interested in publishing with us?
Contact book.department@intechopen.com

Numbers displayed above are based on latest data collected.
For more information visit www.intechopen.com



Chapter

Effect of Ceramic/Graphite Reinforcement on Dry Sliding Wear Behavior of Copper Metal Matrix Hybrid Composites

Manvandra Kumar Singh, Mulkraj Anand, Pushkar Jha and Rakesh Kumar Gautam

Abstract

In the present investigation, effect of ceramic/graphite addition on the dry sliding wear behavior of copper-based hybrid composites have been assessed at three different normal loads of 9.81, 19.62 and 29.43 N. Wear test is performed by using pin-on-disc test rig at sliding speeds of 1.30 and 1.84 m/s under ambient conditions. The copper-based hybrid composites are successfully synthesized by using stir casting route. The samples are characterized by various techniques such as X-rays diffraction (XRD), high resolution-scanning electron microscopy (HR-SEM), scanning electron microscope (SEM) equipped with energy dispersive analysis of X-ray spectroscopy (EDAX). Microstructural investigations reveal the presence of the WC, TiC and graphite particles in the hybrid composites. It is observed that graphite reinforced hybrid composite shows better wear resistance than hybrid composite without graphite addition. In all the cases cast copper specimen shows highest wear rate. The observed friction and wear behavior have been explained on the basis of the presence tribofilm on the worn surface. Microstructural characterization of the worn surface and wear debris show that the mechanism of wear is primarily adhesive and oxidative in case of cast copper, where as it is a mix of adhesive and abrasive wear in case of hybrid composites. Wear debris analysis also helps to understand the wear mechanism involved during dry sliding.

Keywords: metal matrix composites, friction, wear, tribofilm, dry-sliding

1. Introduction

During the last two decades, metal matrix composites (MMCs) have gained researcher's focus due to its outstanding properties such as high elastic modulus, specific strength, specific stiffness, desirable coefficient of thermal expansion, high temperature resistance, and better wear resistance [1, 2]. Among the existing metal matrix composites, copper based composites are gaining enormous importance due to its various automobile and industrial applications viz. automobile radiators, bearings and bushings, heat exchangers, electrical sliding contacts and resistance welding electrodes [3–5]. Copper based composites can be developed by using various techniques viz. stir casting, powder metallurgy, chemical vapor

deposition, etc. However, among these techniques, stir casting technique has an edge over other fabrication techniques [6]. Researchers have reinforced various ceramics such as SiC, TiC, WC, Al_2O_3, graphite and TiB_2, etc. into the copper matrix to enhance its mechanical and tribological properties [7–12]. Kumar and Mondal [13] prepared graphite reinforced copper matrix composites and explored its friction and wear properties at normal loads of 10–55 N and constant velocity of 0.77 m/s by using pin-on-disk. It was noticed that graphite reinforced composites showed improved wear resistance and lower friction coefficients compared to unreinforced copper. The friction and wear resistance improvements are mainly caused due to the formation of a solid self-lubricating film formed by the presence graphite particles. Gautam et al. [14] prepared Cu-Cr-graphite composite through solidification processing. Dry sliding test was conducted at different normal loads 10, 20, 30, and 40 N and a constant sliding speed of 0.786 m/s. It was observed that wear rate of graphite reinforced composites are lower than other composites. It was also observed that average coefficient of friction is reciprocal with the normal load and the graphite added composite reveals the lesser average coefficient of friction. Nayak et al. [15] developed graphite and TiC reinforced copper hybrid composites. It was noticed that hardness of the composites decreases with graphite addition while its hardness increases with TiC addition. Wear test was conducted using a pin- on-disk test rig. Worn surface investigation shows that the reinforcement of TiC and graphite considerably enhances the tribological properties of the copper composites. Rajkumar and Aravindan [16] revealed the tribological behavior of Cu-TiC-graphite hybrid composites under the conditions (normal loads of 12–48 N; and sliding speeds of 1.25–2.51 m/s). It was noticed that the addition of higher graphite content helps to form a mixed smooth layer that enhances the wear resistance and decreases the friction coefficient.

From the literature review it can be concluded that several researchers have studied and reported the various mechanical and tribological behavior of Cu-based hybrid composites. However, only few reports are available for exploring the friction and wear behavior of the graphite along with two ceramics (WC and TiC) reinforced in the copper matrix. Hence, in the present investigation the main focus is to explore the dry sliding wear behavior of graphite reinforced Cu-based hybrid composites by using pin on disk test rig. Further, various characterization techniques were employed to examine the worn surface and wear debris morphologies.

2. Experimental details

Small pieces of commercially (99.99%) pure copper in calculated amount were taken in a graphite crucible and placed in the electric muffle furnace. The temperature of the furnace was set to 1200°C with heating rate of 300°C/h and holding time at this temperature of furnace was set for 30 min. As the furnace temperature attained the temperature of 1200°C, copper pieces in graphite crucible completely changed into molten metal state and then fixed amount of chromium (2 wt%) was added into the melt. Reinforcements such as WC, TiC and graphite in calculated amounts as given in **Table 1** were poured into the molten metal by wrapping in copper foil as small packets with the help of tong and continuously stirred at 300 rpm for 5 min. **Figure 1** presents the SEM morphology of the reinforcing particles (WC, TiC and graphite). **Figure 1(a)** and **(b)** reveals the equiaxed, regular shape and size of WC and TiC. **Figure 1(c)** presents the equiaxed and flake type geometry of the graphite particles. Reinforcements were preheated at temperature of 100°C to make it moisture free. Three compositions were obtained after casting; (a) cast copper, (b) Cu-2 wt% Cr-1.5 wt% WC-1.5 wt% TiC and (c) Cu-2 wt% Cr-1.5 wt%

S. no.	Materials	Compositions	Wt%	Minimum assay	Wt in (g)	Wt in (g) after assay correction
1.	Cast commercial copper	Commercial copper (CC)	100.0	99.5%	1000.0	1005.0
2.	Hybrid composite-1 (HC-1)	Commercial copper (CC)	95.0	99.5%	950.0	954.7
		Tungsten carbide (WC)	1.5	98.0%	15.0	15.3
		Titanium carbide (TiC)	1.5	98.5%	15.0	15.2
		Chromium (Cr)	2.0	99.0%	20.0	20.2
3.	Hybrid composite-2 (HC-2)	Commercial copper (CC)	90.0	99.5	900.0	904.5
		Titanium carbide (TiC)	1.5	98.0	15.0	15.3
		Tungsten carbide (WC)	1.5	98.5	15.0	15.2
		Chromium (Cr)	2.0	99.0	20.0	20.2
		Graphite	5.0	98.0	50.0	51.0

Table 1.
Compositional details of the developed materials.

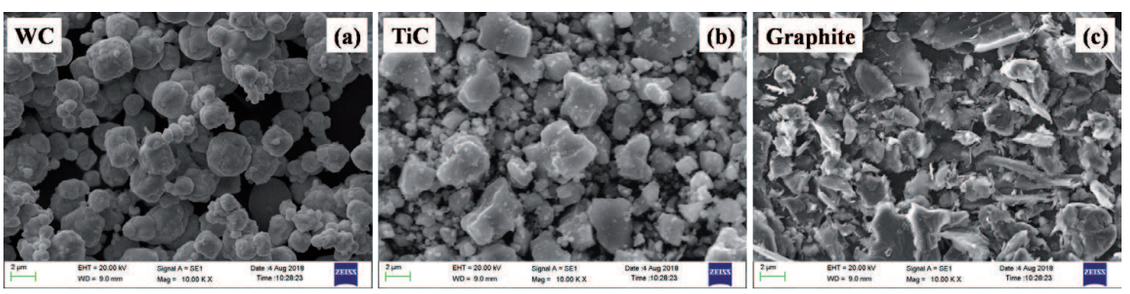


Figure 1.
SEM micrographs of as received (a) WC, (b) TiC and (c) graphite powders.

WC-1.5 wt% TiC-5 wt% Gr and these were designated as CC, HC-1, and HC-2, respectively. After stirring of the molten materials, it was poured into a permanent steel mold and kept for air cooling. After cooling, the developed cast ingot of matrix and hybrid composites were used for different characterizations.

The phase evolution of the hybrid composites were studied by using Rigaku miniflex600 with DTEX-ultra diffractometer with Cu-Kα radiation (λ = 1.54A°). High resolution scanning electron microscope (FEI Netherlands, NOVA NANOSEM450) and scanning electron microscope (ZEISS-EVO/18) equipped with EDAX were utilized for microstructural examinations. Brinell hardness test was performed as per ASTM E10-00 standards, using a load of 500 kg and a 10 mm ball indenter at room temperature. The average of five measurements was reported to ascertain reproducibility.

Friction and wear test of both cast copper and hybrid composites were conducted according to the ASTM G99-05 standards using standard pin on disc wear test rig (MAGNUM Bangalore, India) with a counterface of the EN31 steel hardened to 60 ± 3 HRC at an ambient condition. The samples on the test rig, the surface of the hardened steel disc and test pin were thoroughly cleaned with emery paper and acetone to remove any possible traces of grease and other surface contaminants.

The normal loads were 9.81, 19.62, and 29.43 N and the sliding speeds were 1.30 and 1.84 m/s, respectively. The total sliding distance covered during the wear test was ~5000 and ~7000 m. The weight loss was measured prior to and after the test using an electronic balance with an accuracy of 0.0001 mg. Meanwhile, the volume loss of the samples was calculated through weight loss divided by Archimedes' density of the material. The control panel equipped with the tribometer displayed the frictional force. The same was used to calculate the friction coefficient by dividing it by the normal load. Each test for a particular condition of load and speed was conducted thrice. The average value of three tests was reported in the present investigation. The worn surface of the specimens and wear debris were subjected to SEM and EDAX analyses to explore the nature of the wear mechanism.

3. Results and discussion

3.1 X-ray diffraction (XRD)

X-ray diffraction (XRD) pattern of the CC, HC-1 and HC-2 is shown in **Figure 2**. The diffraction peaks present in the developed materials are indexed with XRD-JCPDS database. One can observe the presence of CuO and Cu_2O phases in the XRD spectra and it can be possibly due to the oxidation of the copper at high temperature with residual atmospheric oxygen present in the furnace. However, the peaks of WC and TiC are not distinct and it can be attributed to the lower weight percentage of the reinforcing particles in the copper matrix which may not be in the detactable range of XRD [17].

3.2 Microstructure

Figure 3(a)–(c) shows the HR-SEM microstructure of the CC, HC-1 and HC-2, respectively. **Figure 3(a)** depicts the microstructure of CC, in which the presence of any foreign particles could not be observed. It shows a plane, smooth and homogeneous morphology. However, the microstructure of hybrid composites show some embedded reinforcing particles into the metal matrix. The embedded reinforcing particles resemble with the crystal geometry of WC which is hexagonal and cubic structure of TiC particles, respectively [18]. The typical microstructures of hexagonal and cubic crystal geometry can be observed in **Figure 3(b)**. **Figure 3(c)** shows the microstructure of the HC-2 which depicts the presence of reinforcing particles into the metal matrix that is shown in the inset. The inset particle are magnified and analyzed for its microstructural geometry. It is found that hexagonal and cubical crystal geometry are particularly the crystal geometry of WC and TiC in the matrix as shown in **Figure 3(c-1)** and **(c-2)**, respectively.

Figure 4 presents the EDAX spectrum of developed materials. The EDAX spectrum of the CC, HC-1 and HC-2 are shown in the **Figure 4(a-a′)**, **(b-b′)** and **(c-c′)**, respectively. Very weak intensity peak of carbon and oxygen are observed in the EDAX spectrum of CC as shown in **Figure 4(a′)**. Carbon intensity peak may be attributed to the presence of less impurity of carbon in CC and oxygen intensity peak may be due to the possible oxidation of the CC at high temperature during melting. Atomic and weight percentage of carbon, oxygen and copper are shown in the corresponding table in **Figure 4**. However, **Figure 4(b′)** and **(c′)** show the EDAX spectrum of the HC-1 and HC-2, respectively. From spectrum, comparatively smaller intensity peak of carbon, oxygen, tungsten, titanium and chromium are observed than that of the copper intensity peak. It can be observed that atomic/weight percentage of carbon and oxygen found in hybrid composites are higher

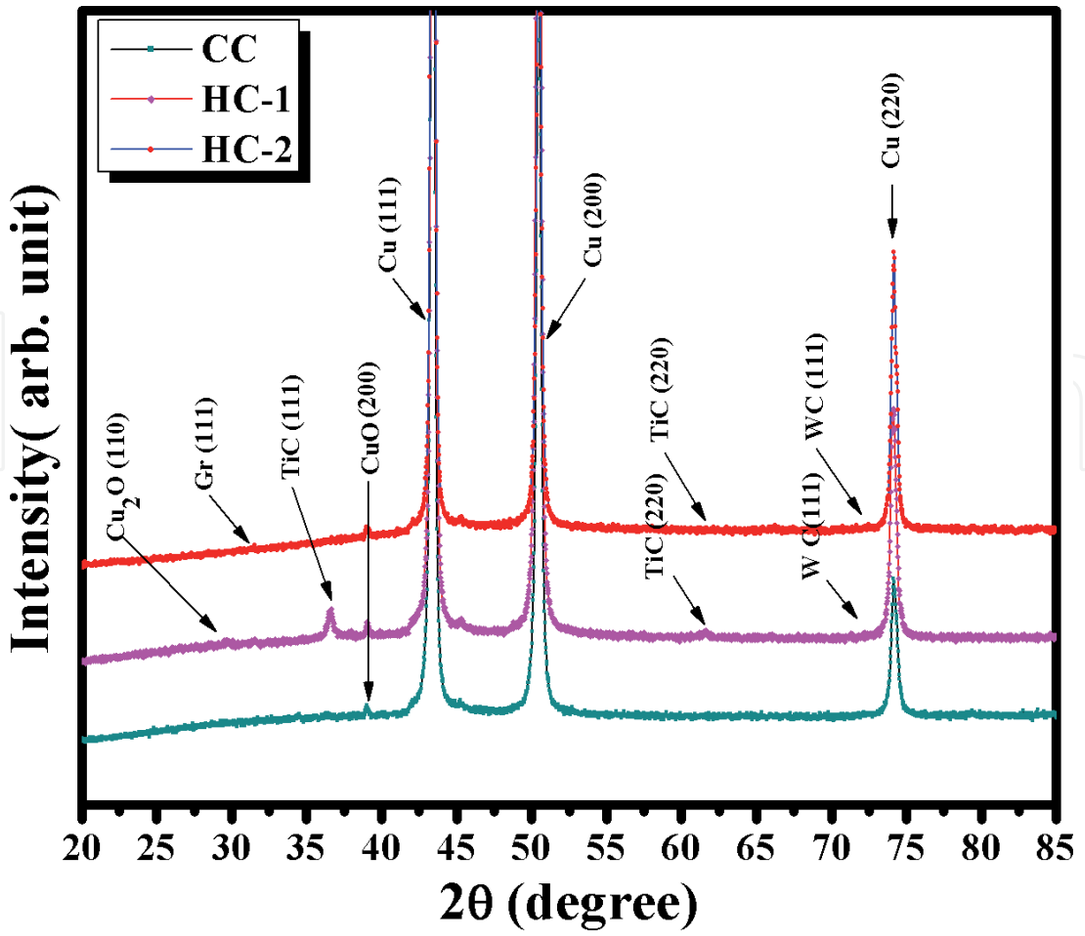


Figure 2.
X-ray diffraction patterns of CC, HC-1 and HC-2 specimens.

than the CC as depicted in the table of **Figure 4(b′)** and **(c′)**. The possible reason for the increased atomic/weight percentage of carbon in EDAX spectrum of composites can be due to the addition of carbon in form of carbides and graphite. It can be concluded from the **Figure 4(b′)** and **(c′)** that the WC, TiC and graphite are added to the commercial copper.

3.3 Density and hardness

The variation in the density of the developed materials is shown in **Figure 5**. It is clear from the figure that HC-1 shows higher density as compared to the CC and HC-2. The reason for the higher density of HC-1 can be credited to the improved bonding between the reinforcement particles and the copper matrix. To enhance the bonding in the hybrid composites, Cr has been used as a wetting agent [14]. It can also be inferred that HC-2 shows lower density than cast copper and HC-1. The possible reason for such lowering in density of HC-2 can be due to the reinforcement of ultralow density graphite particles [19].

Figure 5 also depicts the variation in the hardness of CC, HC-1 and HC-2. It is obvious from the figure that hybrid composites (HC-1 and HC-2) show higher hardness as compared to the cast copper matrix. The reason for the increased hardness of HC-1 and HC-2 can be attributed to the reinforcement of harder WC and TiC ceramics in the ductile copper matrix. During hardness test, when the load is applied through ball indentation on the materials, the applied load transfers from the softer matrix to the harder reinforcing particle and it restricts further plastic deformation. The differences in the elastic modulus and coefficient of thermal expansion of matrix and reinforcement can also have a significant

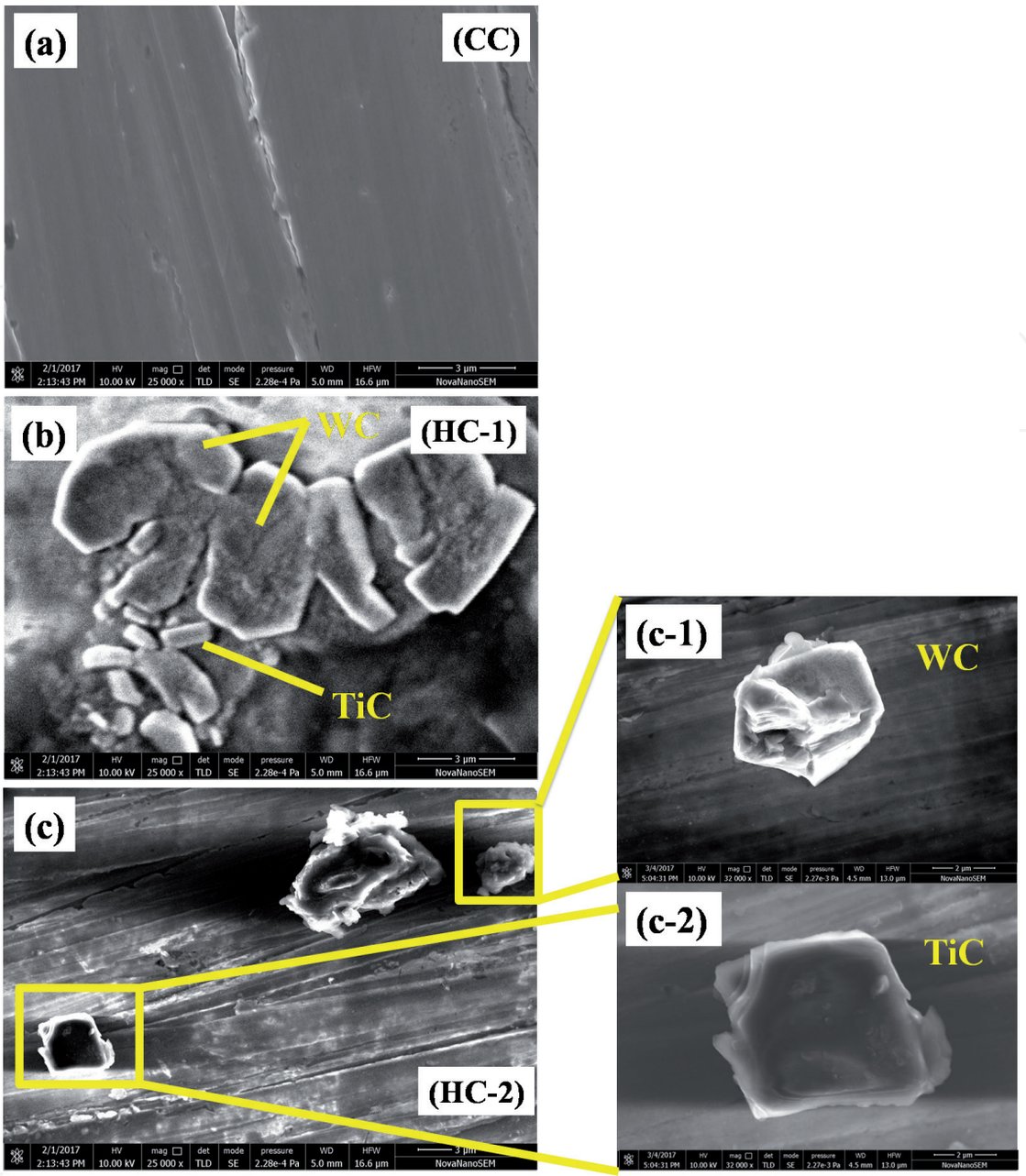


Figure 3.
HR-SEM microstructure of developed materials (a) CC, (b) HC-1, and (c) HC-2.

role in the improvement of hardness of the hybrid composites. In addition, the strain hardening also affects the hardness behavior of the materials [20]. It is observed that HC-1 and HC-2 shows almost 80 and 50% increment in hardness as compared to the copper matrix, respectively. The hardness of the HC-2 is lower as compared to HC-1; this is due to the reinforcement of softer graphite materials in the softer matrix [19].

3.4 Investigation of sliding wear behavior

Figure 6(a)–(f) shows the variation of the cumulative volume loss with the sliding distance for all the materials investigated in the present study under different loads of 9.81, 19.62 and 29.43 N for sliding speed of 1.30 and 1.84 m/s. It can be observed that cumulative volume loss increases as the sliding distance increases for CC, HC-1 and HC-2, respectively. Moreover, the volume loss of CC is higher at all the normal loads as compared to the hybrid composites. Lower volume loss of the

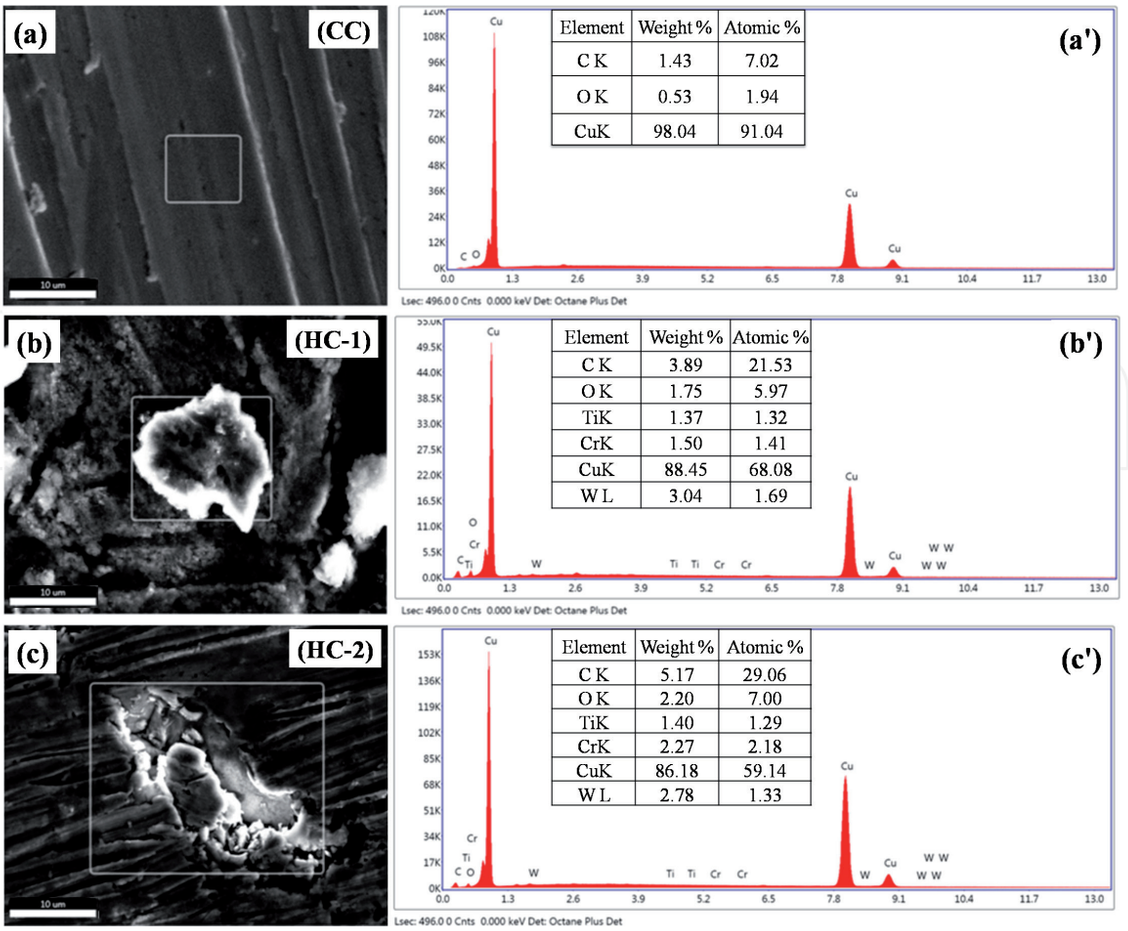


Figure 4.
EDAX spectrum of the marked portion of the micrograph of (a) CC, (b) HC-1, and (c) HC-2.

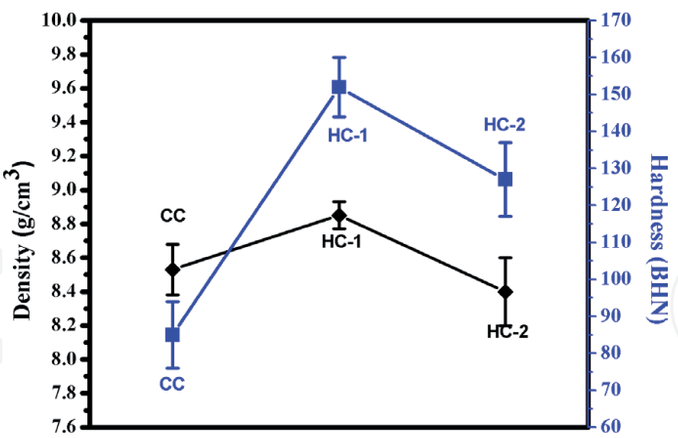


Figure 5.
Variation of density and hardness of the developed materials.

hybrid composites can be credited to the reinforcement of harder particles (TiC and WC) in case of HC-1 because these harder particles provide a shield to the relatively softer matrix during sliding and enhance the load bearing capacity of the hybrid composite [21]. In case of HC-2, the volume loss is minimum and it can be attributed to the combined effect of harder phase (TiC and WC) as well as softer phase (graphite) reinforcement. During sliding, the graphite particles comes out from the surface of the wear pin and act as solid lubricant and develop a thin tribofilm between the wear pin and hard counter surface which reduces the coefficient of friction thus it reduces the volume loss.

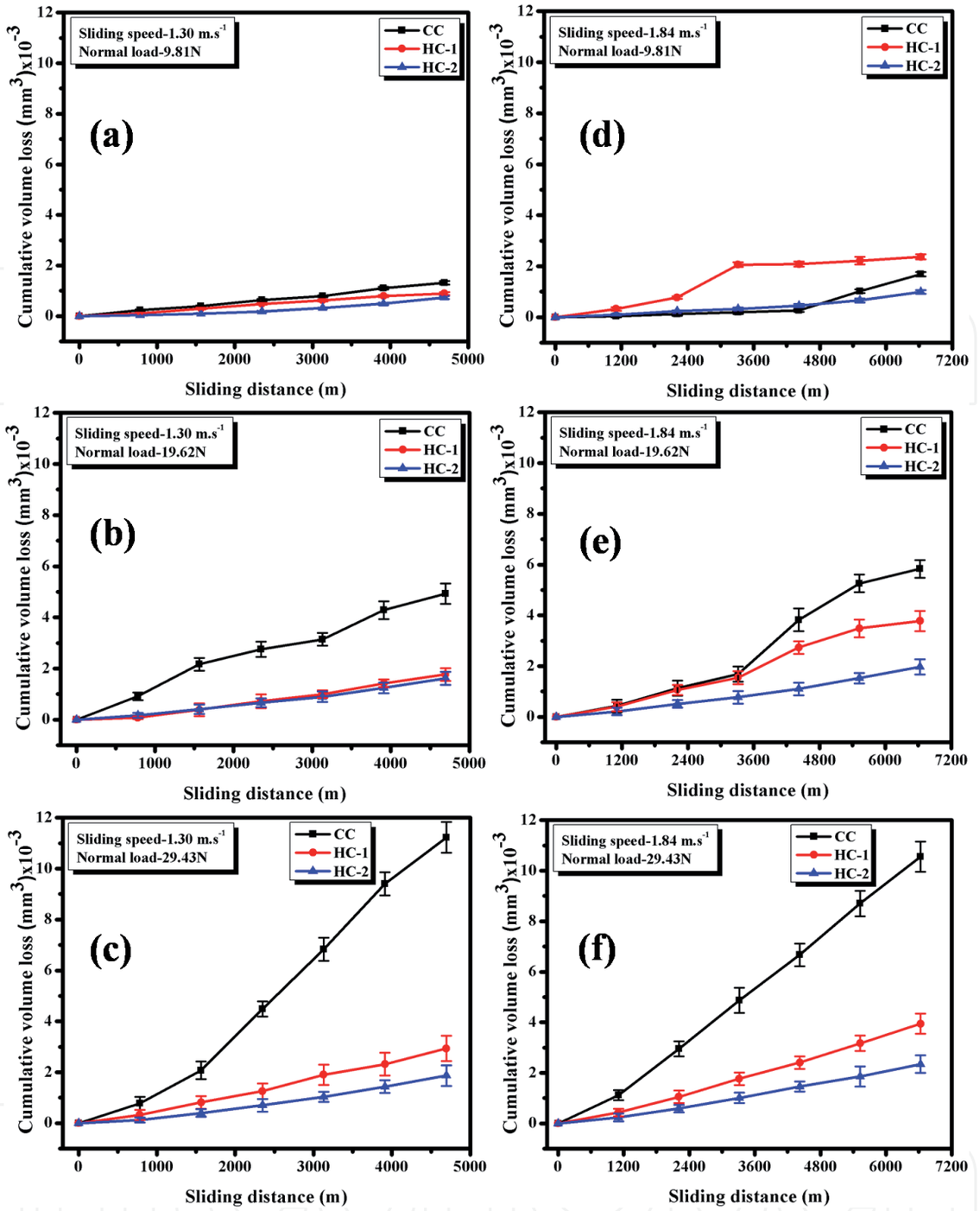


Figure 6.
Variation of cumulative volume loss with sliding distance for CC, HC-1 and HC-2 at 1.30 m/s and at 1.84 m/s.

Figure 7(a) and **(b)** shows the variation of the wear rate with normal load for CC, HC-1 and HC-2 at sliding speed of 1.30 and 1.84 m/s. It is clear from **Figure 7(a)** and **(b)** that the wear rate increases as the load increases at both the sliding speeds. Among the materials investigated, CC shows the highest wear rate and HC-2 shows lowest wear rate. In case of CC, there are chances of direct metal to metal contact and it may lead to adhesive wear. Adhesive wear mechanism initiates plastic deformation which is responsible for the highest wear rate. Similar observations for wear behavior of unreinforced copper were reported by Tu et al. [22]. The wear rate of HC-1 is comparatively lesser than CC because of reinforcement of harder particle like—WC and TiC. During sliding contacts these harder particles get early exposure on the surface of the wear pin and these particles may carry the applied normal load for a longer time without transferring the contacts to copper matrix [23].

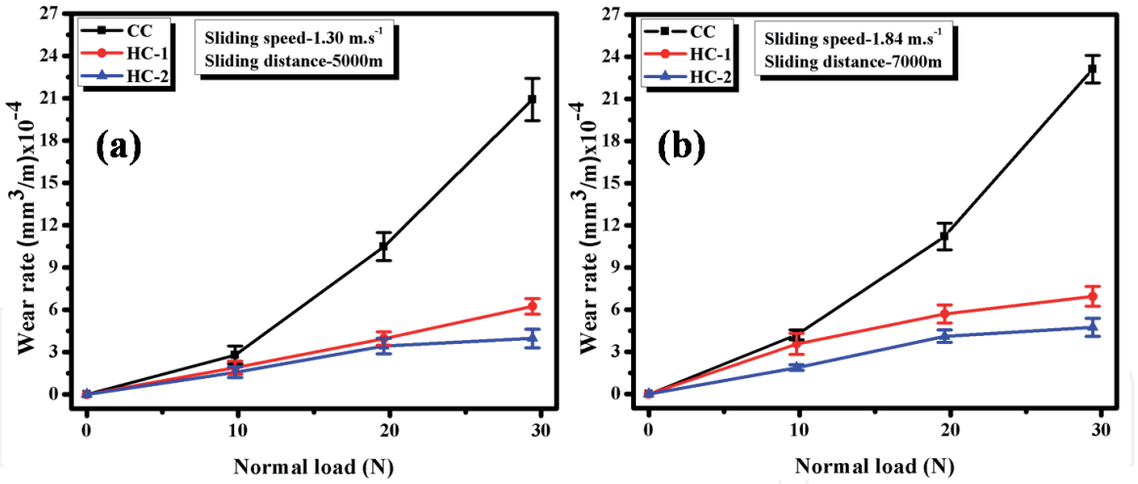


Figure 7.
Variation of wear arte with normal load for CC, HC-1 and HC-2 at (a) 1.30 m/s and (b) at 1.84 m/s.

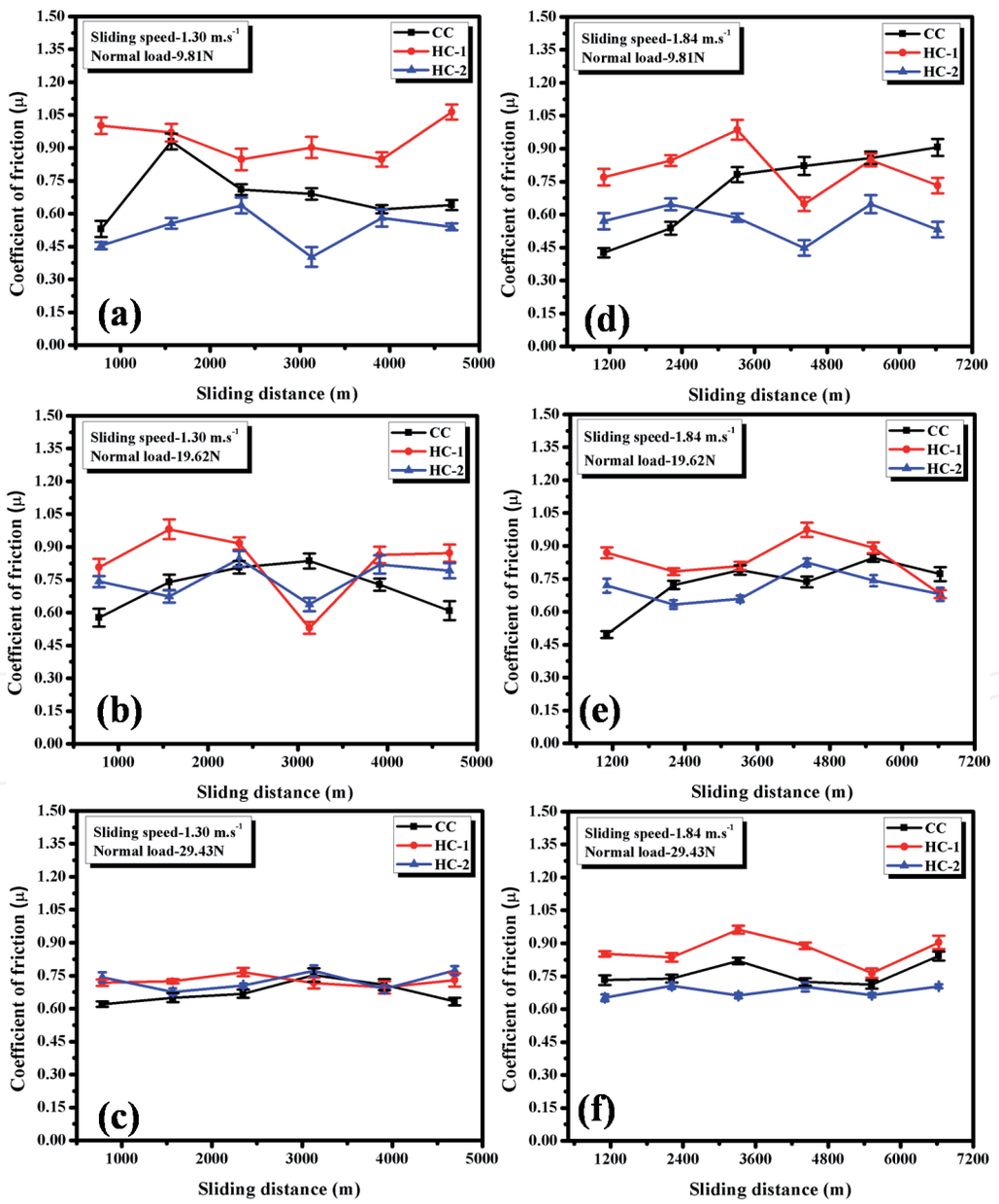


Figure 8.
The variation of coefficient of friction with sliding distance of CC, HC-1 and HC-2 at 1.30 m/s (a)–(c) and at 1.84 m/s (d)–(f).

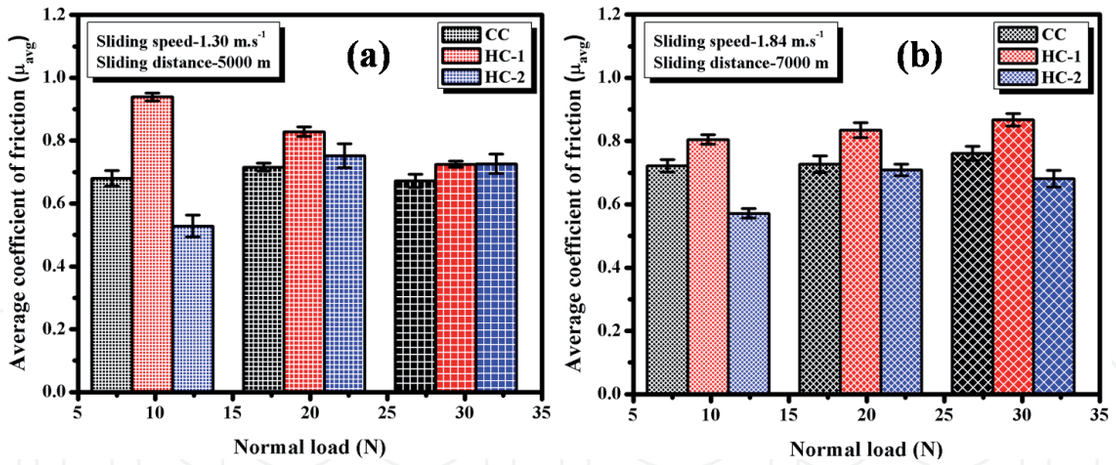


Figure 9.
The variation of the average coefficient of friction with normal load for CC, HC-1 and HC-2 at (a) 1.30 m/s and (b) 1.84 m/s.

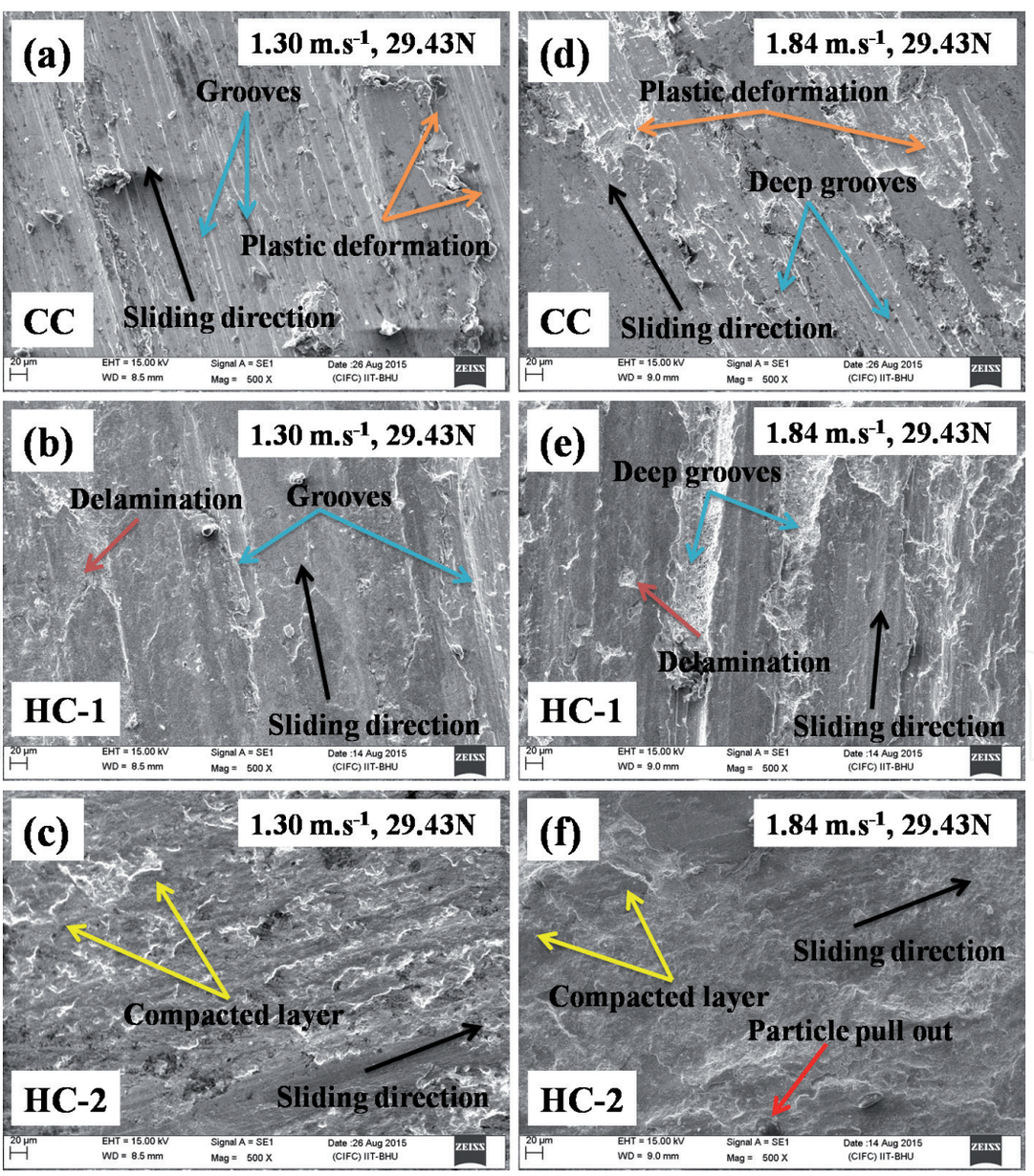


Figure 10.
SEM micrograph of worn surfaces at 29.43 N of (a) CC, (b) HC-1, (c) HC-2 at 1.30 m/s and (d) CC, (e) HC-1, (f) HC-2 at 1.84 m/s.

The wear mechanism changes from adhesive to abrasive nature. It can be observed that HC-2 shows lowest wear rate and the reason can be credited to the combined effect of hard particles reinforcement and squeezing out of the graphite particle. At the highest load the debris particles that comes during sliding, gets compacted between the mating surfaces. This compacted layer of debris which contains the graphite particles help to form a type of tribofilm and it may be responsible for the lowest wear rate [16]. It can be observed from the **Figure 7** that as sliding speed increases from 1.30 to 1.84 m/s the wear rate increases for CC, HC-1 and HC-2. The reason can be attributed to the fact that as sliding speed increases it gives rise to increase in frictional heat energy. The dissipated heat energy makes the matrix surface softens and weakens the interface with allowing easier pull out of the particulates [24].

The typical variation of coefficient of friction with sliding distance for CC, HC-1 and HC-2 at different normal loads (9.81, 19.62 and 29.43 N) and sliding speeds (1.30 and 1.84 m/s) are presented in **Figure 8(a)–(f)**. It is observed that coefficient of friction fluctuates with the sliding distance. The reason for this fluctuation can be due to the disparity in contact that occurs when the sample and the counterface are evolving to develop a better surface conformity. Other reason for the fluctuation of hybrid composites can be credited to the fact that during sliding the abrasive particles comes between the contacting surfaces.

Figure 9(a) and **(b)** show the variation of the average coefficient of friction with normal load for CC, HC-1 and HC-2 at sliding speeds of 1.30 and 1.84 m/s,

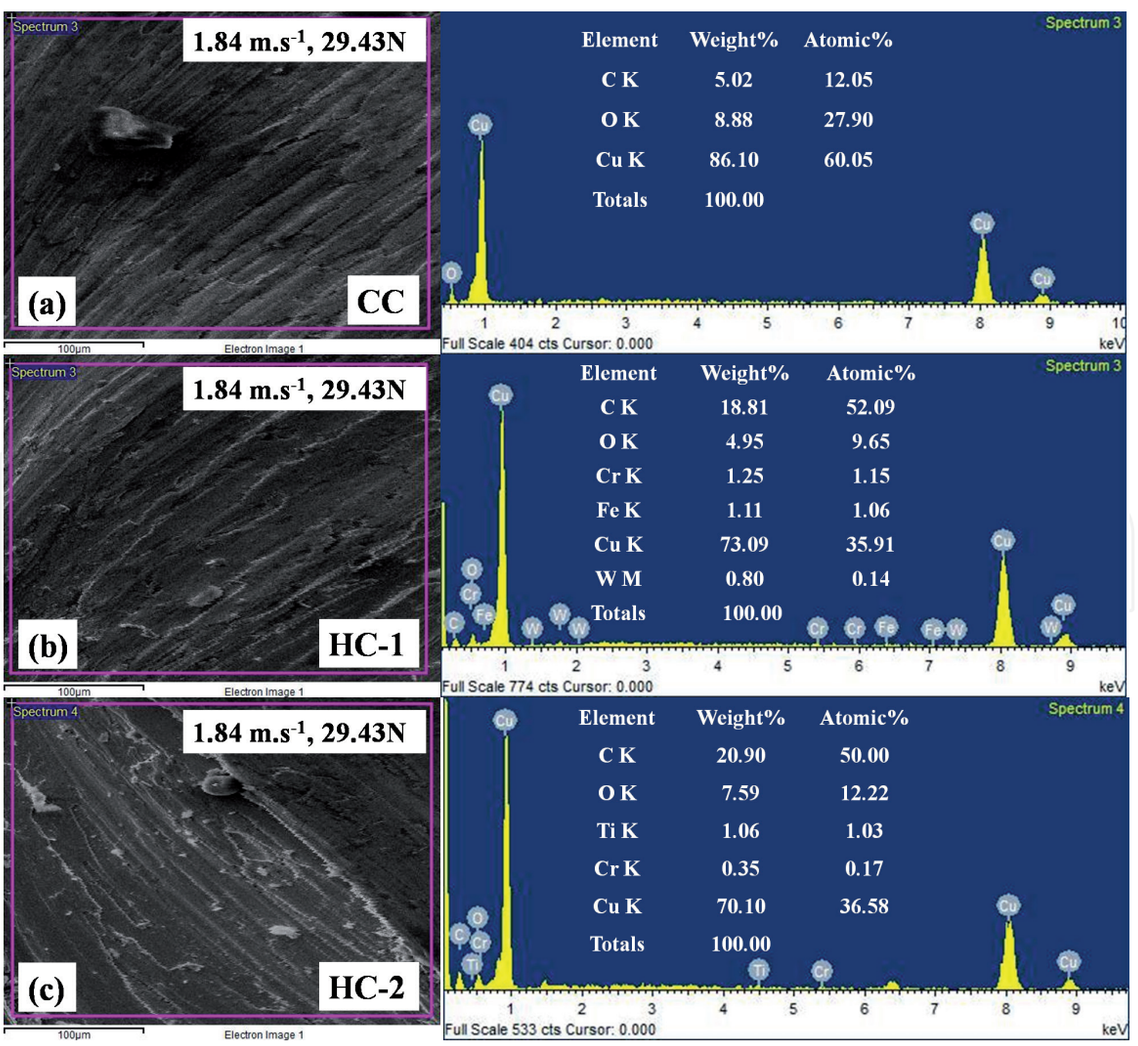


Figure 11.
EDAX spectrum of the worn surface of (a) CC, (b) HC-1, (c) HC-2 at sliding speed of 1.84 m/s and load of 29.43 N.

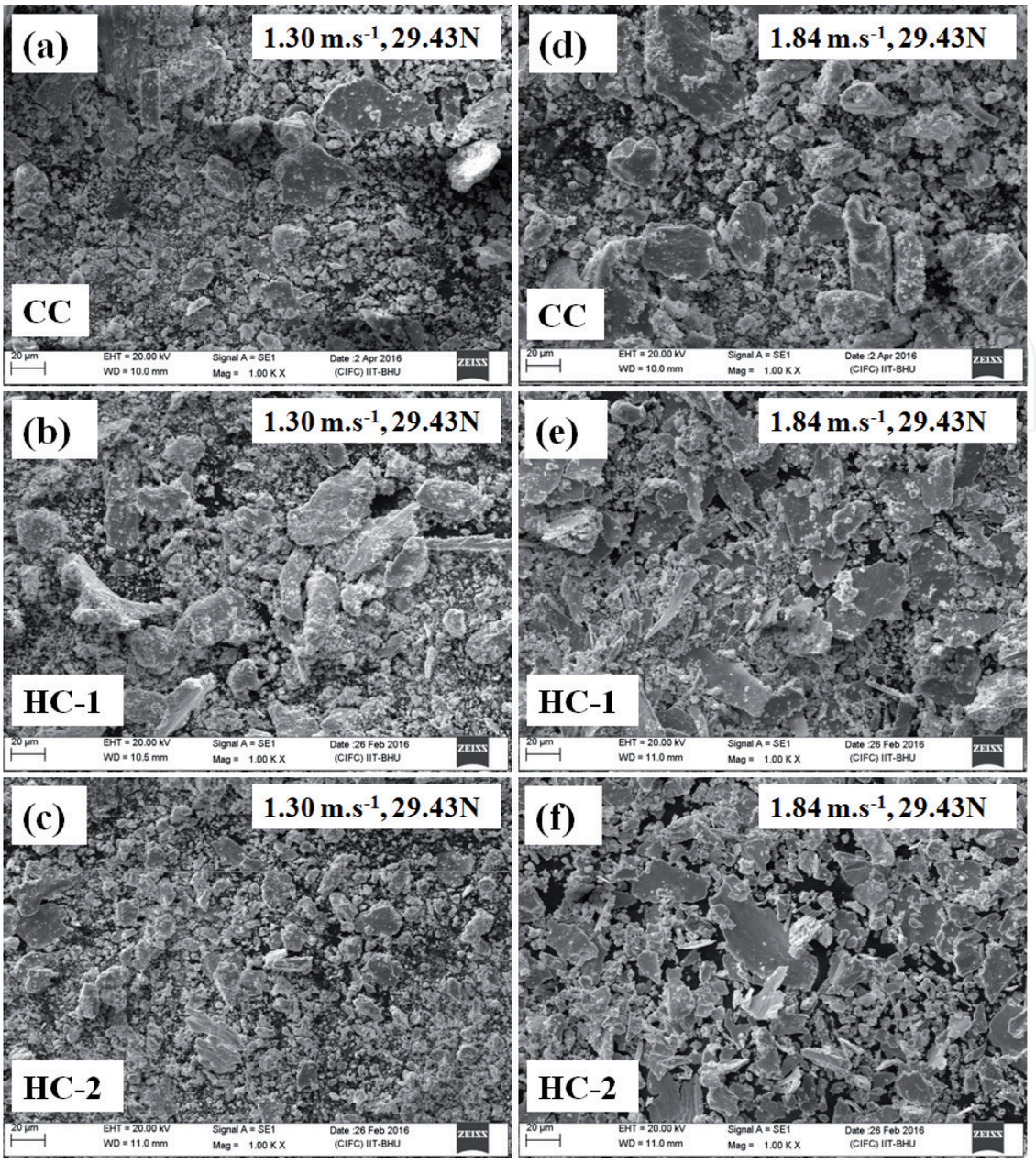


Figure 12.
SEM morphology of wear debris at 29.43 N of (a) CC, (b) HC-1, (c) HC-2 at 1.30 m/s and (d) CC, (e) HC-1, (f) HC-2 at 1.84 m/s.

respectively. It can be observed that HC-1 shows the highest coefficient of friction among all investigated materials at both the sliding speeds. It can also be observed that coefficient of friction increases as load increases from 9.81 to 29.43 N. The reason for the highest coefficient of friction of HC-1 can be credited to the reinforcement of ceramic particles and these particles when comes between the contacting surfaces may give rise to three body abrasion and thus coefficient of friction increases [25]. As the load increase the surface contact increases and thus more surface asperities come in contact and it can be the reason for the increase in the coefficient of friction for the materials. However, one can observe that HC-2 shows lower coefficient of friction than CC and HC-1. The possible reason for this can be due to the presence of softer phase graphite particles which reduces the coefficient of friction in all the cases due to the formation of the tribofilm. The tribofilm works as a lubricating layer and reduces the coefficient of friction with the sliding distance [26].

Figure 10(a)–(f) show the SEM micrographs of worn surfaces of CC, HC-1 and HC-2 at maximum normal load of 29.43 N and sliding speeds of 1.30 and 1.84 m/s,

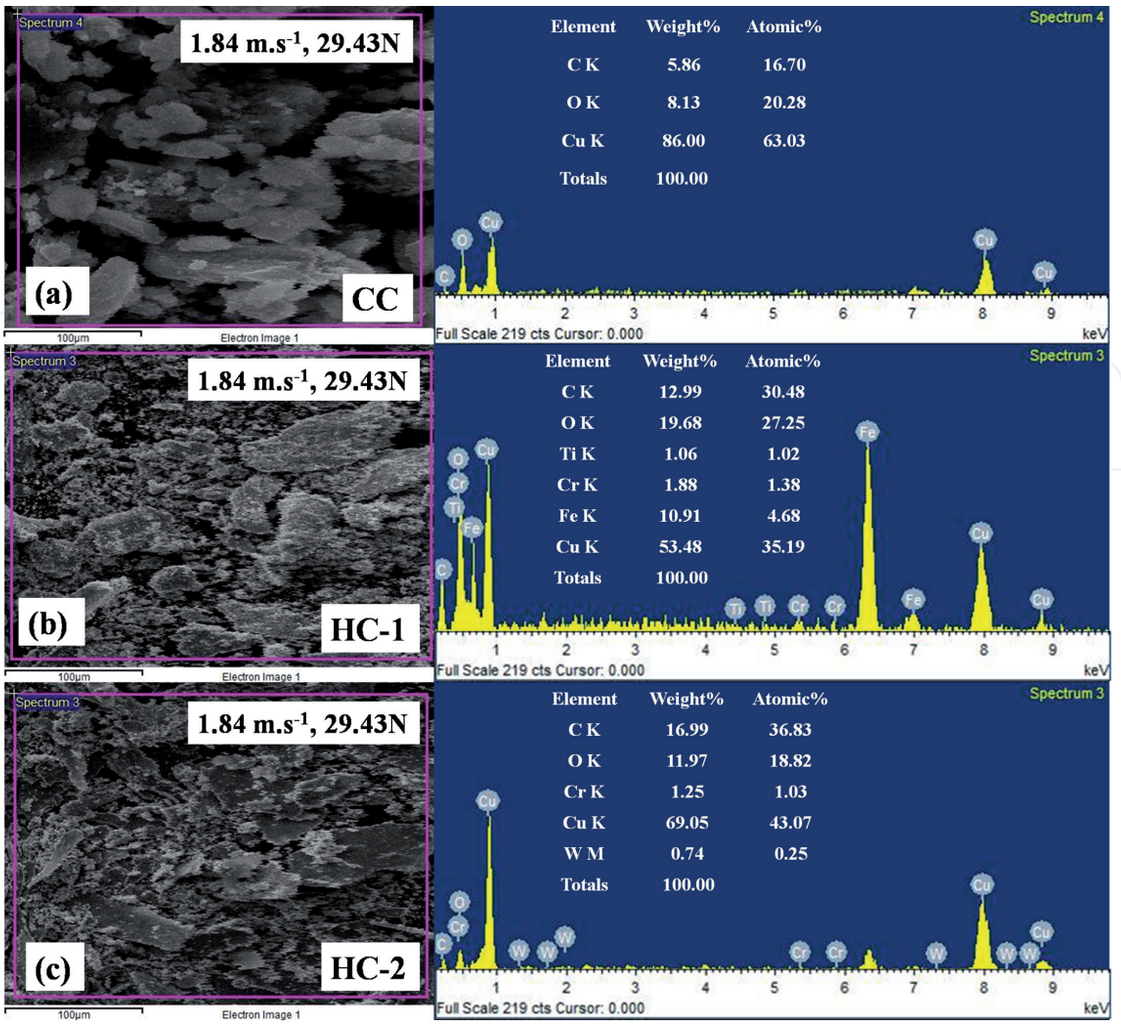


Figure 13.
EDAX spectrum of wear debris of (a) CC, (b) HC-1 and (c) HC-2 at sliding speed of 1.84 m/s and load of 29.43 N.

respectively. The corresponding SEM micrographs of the CC worn surface shown in **Figure 10(a)** and **(d)** exhibit the presence of the grooves due to the adhesive wear mechanism which attributed to the direct metal to metal contact. Due to the adhesive wear plastic deformation can be observed at the worn surfaces. One can observe that grooves are less deep in **Figure 10(a)** at lower sliding speed of 1.30 m/s as compared the grooves appearing in **Figure 10(d)** at higher sliding speed of 1.84 m/s. **Figure 10(b)** and **(e)** show the worn surface of HC-1 at both the sliding speeds. The grooves along with some delamination can be observed in the micrograph shown in **Figure 10(b)**. Similarly, **Figure 10(e)** shows the deeper grooves with delamination at higher sliding speed of 1.84 m/s. The micrographs predict that there is transformation of wear mechanism from adhesive to abrasive wear in case of HC-1 hybrid composite. The abrasive actions are mainly caused by the wear debris that mainly contains traces of reinforced ceramic particles. Due to the abrasive wear mechanism in case of HC-1 as shown in the **Figure 10(b)** and **(e)** it can be confirmed that the results given in **Figure 9** are convincing. The worn surface of HC-2 is shown in **Figure 10(c)** and **(f)** which shows less grooves and mild wear region as compared to CC and HC-1at both the sliding speeds. The presence of lesser or no grooves on the worn surfaces at both the sliding speeds for HC-2 can be due to the reason that these worn surfaces may be covered by the transfer layer as depicted in the micrograph. This layer is basically formed from the wear debris coming out during sliding. When this transfer layer gets compacted during sliding, because heat is generated during sliding, then it protects the surface against wear and thus wear rate decreases as

shown in **Figure 7** [27]. In **Figure 10(f)**, particles pullout can be seen which comes from the wear pin during sliding and these particles may create a lubricating surface which comes between the sliding surfaces and defends the surface against wear. This layer also inhibits a direct metal–metal contact and provides a low shearing strength junction at the interface, thereby resulting in a reduced friction coefficient in comparison to the hybrid composites as shown in **Figure 9**.

Figure 11(a)–(c) shows the typical EDAX spectrum of the marked portion in worn surface of CC, HC-1, HC-2 at sliding speed of 1.84 m/s and normal load of 29.43 N respectively. **Figure 11(b)** displays the presence of Fe in the EDAX spectra of HC-1which confirms that the metal transfer occurred from the counter face. The presence of oxygen in the spectra indicates the possibility of oxidation that might have occurred during sliding possibly due to increase in contacting surfaces.

The wear debris analysis helps to predict the wear mechanism involved during dry sliding. **Figure 12** shows SEM morphology of wear debris of (a) CC, (b) HC-1, (c) HC-2 at normal load of 29.43 N and at sliding speed of 1.84 m/s. It can be observed that wear debris particle appearing in **Figure 12(a)** are larger in size which got detached from the CC due to adhesive wear mechanism and thus plastic deformation occurs. One can also observe that **Figure 12(b)** which corresponds to the wear debris of HC-1 appears like plate and flake shaped. The reason can be attributed to an abrasive micro-cutting effect. The other cause for the smaller wear debris is due to the higher hardness of HC-1. **Figure 12(c)** shows equiaxed sheets and powder like morphology. Similar observations were reported by Sundararajan and Rajadurai [28]. This type of morphology predicts that wear is lesser and thus the debris particles are smaller. In this case it can be predicted that these fine debris particles acts as lubricant during sliding.

Figure 13 shows the EDAX spectrum of the wear debris of CC, HC-1 and HC-2 at normal load of 29.43 N and sliding speed of 1.84 m/s. EDAX spectrum of wear debris shows the intensity peak of entire reinforcing elements with their atomic and weight % that are shown in the spectrum. The greater amount of weight and atomic % of oxygen are observed in the entire EDAX spectrum of wear debris compared to EDAX spectrum of developed materials. Such increment in oxygen % in EDAX spectrum of wear debris indicates the involvement of oxidative wear of the materials during dry sliding. The intensity peak of iron element is observed in the EDAX spectrum of wear debris of HC-1 at both the sliding speeds. It is attributed to the higher hardness of the HC-1 which abrades the counter steel disc in lesser amount and adheres with the other wear debris. The analysis of EDAX spectrum of the wear debris confirms that mainly oxidative, abrasive and adhesive wear mechanism takes place during dry sliding.

4. Conclusions

- Copper-based hybrid composites have been successfully synthesized by using stir casting route. XRD pattern confirms that TiC, WC, and graphite are present in the hybrid composites.

- Microstructural analysis reveals the presence of reinforcing particles and its uniform distribution. Density of the HC-2 is lowest. However, the hardness of the HC-1 is found to be maximum.

- The volume loss of CC is higher at all the normal loads as compared to the hybrid composites. CC shows highest wear rate among the developed specimens. HC-2 shows better wear resistance than HC-1. This has been attributed

to the lubricating effect of graphite that forms tribofilm between the contacting surfaces during sliding.

- It is observed that there are no certain trends of coefficient of friction with sliding distance for CC, HC-1 and HC-2 hybrid composites. It can also be observed that HC-2 shows lower coefficient of friction than CC and HC-1. The possible reason for this can be due to the presence of softer phase graphite particles which reduces the coefficient of friction in all the cases.

- Worn surface analysis predicts that the mechanism of wear is primarily adhesive and oxidative in case of CC where as it is a mix of adhesive and abrasive wear in case of hybrid composites.

- EDAX spectra confirm that the metal transfer occurred from the counter face in case of hybrid composites. The presence of oxygen in the spectra indicates the possibility of oxidation that might have occurred during sliding. Wear debris analysis also helps to understand the wear mechanism.

Author details

Manvandra Kumar Singh[1*], Mulkraj Anand[2], Pushkar Jha[3] and Rakesh Kumar Gautam[2]

1 Department of Mechanical Engineering, Mewar University, Chittorgarh, India

2 Department of Mechanical Engineering, Indian Institute of Technology (BHU), Varanasi, India

3 School of Mechanical Engineering, KIIT Deemed to be University, Bhubaneswar, India

*Address all correspondence to: mksingh.rs.mec13@itbhu.ac.in

IntechOpen

© 2019 The Author(s). Licensee IntechOpen. Distributed under the terms of the Creative Commons Attribution - NonCommercial 4.0 License (https://creativecommons.org/licenses/by-nc/4.0/), which permits use, distribution and reproduction for non-commercial purposes, provided the original is properly cited. BY–NC

References

[1] Miracle DB. Metal matrix composites from science to technological significance. Composites Science and Technology. 2005;**65**:2526-2540

[2] Ralph B, Yuen HC, Lee WB. The processing of metal matrix composites—An overview. Journal of Materials Processing Technology. 1997;**63**:339-353

[3] Heringhaus F, Raabe D. Recent advances in the manufacturing of copper-base composites. Journal of Materials Processing Technology. 1996;**59**:367-372

[4] Sapate SG, Uttarwar A, Rathod RC, Paretkar RK. Analyzing dry sliding wear behaviour of copper matrix composites reinforced with pre-coated SiCp particles. Materials and Design. 2009;**30**:376-386

[5] Mai YJ, Chen FX, Lian WQ, Zhang LY, Liu CS, Jie XH. Preparation and tribological behavior of copper matrix composites reinforced with nickel nanoparticles anchored graphene nanosheets. Journal of Alloys and Compounds. 2018;**756**:1-7

[6] Hashim J, Looney L, Hashmi MSJ. Metal matrix composites: Production by the stir casting method. Journal of Materials Processing Technology. 1999;**92-93**:1-7

[7] Celebi Efe G, Ipek M, Zeytin S, Bindal C. An investigation of the effect of SiC particle size on Cu–SiC composites. Composites: Part B. 2012;**43**:1813-1822

[8] Akhtar F, Askari SJ, Shah KA, Du X, Guo S. Microstructure, mechanical properties, electrical conductivity and wear behavior of high volume TiC reinforced Cu-matrix composites. Materials Characterization. 2009;**60**:327-336

[9] Hong E, Kaplin B, You T, Suh M-s, Kim Y-S, Choe H. Tribological properties of copper alloy-based composites reinforced with tungsten carbide particles. Wear. 2011;**270**:591-597

[10] Besterci M, Kohú I, t, Velgosova O. Microstructural parameters of dispersion strengthened Cu–Al_2O_3 materials. Journal of Materials Science. 2008;**43**:900-905

[11] Ma W, Lu J, Wang B. Sliding friction and wear of Cu–graphite against 2024, AZ91D and Ti6Al4V at different speeds. Wear. 2009;**266**:1072-1081

[12] Dinaharan I, Saravanakumar S, Kalaiselvan K, Gopalakrishnan S. Microstructure and sliding wear characterization of Cu/TiB_2 copper matrix composites fabricated via friction stir processing. Journal of Asian Ceramic Societies. 2017;**5**(3):295-303

[13] Kumar J, Mondal S. Microstructure and properties of graphite-reinforced copper matrix composites. Journal of the Brazilian Society of Mechanical Sciences and Engineering. 2018;**40**:196

[14] Gautam RK, Ray S, Sharma SC, Jain SC, Tyagi R. Dry sliding wear behavior of hot forged and annealed Cu–Cr–graphite in-situ composites. Wear. 2011;**271**:658-664

[15] Nayak D, Ray N, Sahoo R, Debata M. Analysis of tribological performance of Cu hybrid composites reinforced with graphite and TiC using factorial techniques. Tribology Transactions. 2014;**57**:908-918

[16] Rajkumar K, Aravindan S. Tribological performance of microwave sintered copper–TiC–graphite hybrid composites. Tribology International. 2011;**44**:347-358

[17] Cullity BD. Elements of X-Ray Diffraction. 2nd ed. London, UK: Addision Wesley; 1978

[18] Singh MK, Gautam RK. Synthesis of copper metal matrix hybrid composites using stir casting technique and its mechanical, optical and electrical behaviours. Transactions of the Indian Institute of Metals. 2017;**70**:2415-2428. DOI: 10.1007/s12666-017-1103-0

[19] Rajkumar K, Aravindan S. Microwave sintering of copper–graphite composites. Journal of Materials Processing Technology. 2009;**209**:5601-5605

[20] Rajkovic V, Bozic D, Stasic J, Wang H, Jovanovic MT. Processing, characterization and properties of copper-based composites strengthened by low amount of alumina particles. Powder Technology. 2014;**268**:392-400

[21] Jha P, Gautam RK, Tyagi R. Friction and wear behavior of Cu–4 wt.%Ni–TiC composites under dry sliding conditions. Friction. 2017;**5**:437-446. DOI: 10.1007/s40544-017-0157-7

[22] Tu JP, Rong W, Guo SY, Yang YZ. Dry sliding wear behavior of in situ Cu–TiB_2 nanocomposites against medium carbon steel. Wear. 2003;**255**:832-835

[23] Kumar A, Jha PK, Mahapatra MM. Abrasive wear behavior of in situ TiC reinforced with Al-4.5%Cu matrix. Journal of Materials Engineering and Performance. 2014;**23**:743-752

[24] Prabhu TR, Varma VK, Vedantam S. Tribological and mechanical behavior of multilayer Cu/SiC + Gr hybrid composites for brake friction material applications. Wear. 2003;**255**:832-835

[25] Jha P, Gautam RK, Tyagi R, Kumar D. Sliding wear behavior of TiC-reinforced Cu-4 wt.% Ni matrix composites. Journal of Materials Engineering and Performance. 2016;**25**:1-9

[26] Sarmadi H, Kokabi AH, Reihani SMS. Friction and wear performance of copper–graphite surface composites fabricated by friction stir processing (FSP). Wear. 2013;**304**(1):1-12

[27] Saka N, Teixeira JJP, Suh NP. Wear of two phase metals. Wear. 1977;**44**:77-86

[28] Sundararajan S, Rajadurai JS. Investigation of microstructure, mechanical, and tribological properties of solid self-lubricating copper hybrid composites processed by solid-state mixing technique. Proceedings of the Institution of Mechanical Engineers, Part J: Journal of Engineering Tribology. 2016;**230**:40-56